Properties of xYSZ nanoparticles and pellets with x varying from 1 to 15%

C. Suciu* E. Dorolti** and A. C. Hoffmann***

* CMR-Prototech, Fantoftveien 38, 5892, Bergen, Norway, crina.ilea@prototech.no
**Faculty of Physics, Babes-Bolyai University, 400084, Cluj–Napoca, Romania
*** Dept. of Phys. and Techn., Univ. of Bergen, Allegt. 55, 5007 Bergen, Norway,nfyah@uib.no

ABSTRACT

Analyses of a series of xYSZ materials, where x varies from 1–15%, both in powder form and after sintering to ion-conducting ceramics for use in SOFC fuel cells have been carried out. XRD analyses show the nanoparticles to be in the cubic structure, confirming the stabilization of this crystal structure in nanocrystals. XRD also show that all the interatomic distances in the materials increased with increasing doping. For the sintered materials the relative densities exhibited a minimum at around 8% doping. In spite of this minimum, EIS analyses indicate that both the grain interior and grain boundary contributions to the material resistivity are the smallest at around 8% doping.

Keywords: nanoparticles, grain boundaries, sintering, ionic conductivity, fuel cells, YSZ.

1 INTRODUCTION

The ionic conductivity of yttria-doped zirconia (YSZ) is interesting due to their use in solid oxide fuel cells (SOFCs), mainly as electrolyte materials, but also for mixing, in the form of micro- or nanosized particles, into the anode to create a zone in the anode containing both electronically and ionically conducting grains to extend the triple-phase-boundary (TPB) accessible to all three types of species necessary for the anodic electrode reaction:

$$O^{2-} + H_2 \rightarrow H_2O + 2e^- \quad (1)$$

to proceed, namely oxygen ions, electrons and gaseous hydrogen and water. The use of YSZ nanoparticles in the inner region of the anode will increase the extent of the TPB. Furthermore, production of SOFC electrolytes using nano-particle precursors offer new possibilities for designing the grain structure.

Another important application of SOFCs is generation of hydrogen, e.g. as an energy carrier by reversing the operation of the cell.

Doping of zirconia with yttria both stabilizes a cubic crystal structure and creates one oxygen vacancy for every two tetravalent zirconium ions substituted with trivalent yttrium ions. The ionic conductivity of the material is due to oxygen ions hopping between these vacancies.

Statistically, one would expect maximal ionic conductivity to occur when half of the oxygen positions are vacancies, but mutual interference and ordering effects causes the maximal conductivity to be at much lower doping levels, namely of around 8 mol%, referred to as 8YSZ [1].

Nevertheless it is interesting for a number of reasons to know the crystal structure and the conductivity of YSZ materials as a function of the doping level around this optimum. For example, materials with doping levels other than 8 mol% have mechanical properties different from, and better than 8YSZ.

The objective of this work was to synthesize and characterize nanoparticles of xYSZ with x varying in the range 1–15% and to sinter the powders into pellets, analyzing the grain structure and the effects of this structure on the electrical properties of the pellets [2].

2 EXPERIMENTAL METHODS

The YSZ nanoparticles were synthesized using the sol-gel principle by hydrolysis and condensation reactions using new, cost effective and environmentally friendly precursors in a process developed by the authors [3]. The role of the organic precursors in forming particles of optimal properties is discussed in reference [4].

The pellets were obtained by pressing the powder in a uni-axial press at 600 Bars followed by further pressing in a cold isostatic press (CIP) at 1200 Bars for 2 minutes. The sintering program for the pressed pellets was as follows: heating at a rate of 100°C/h up to 1500°C followed by a dwell time of 10 h and cooling at a rate of 150°C/h down to 20°C.

The nanoparticles and the sintered pellets were characterized in the following ways:

- The specific surface area (SSA) and particle size were measured via nitrogen adsorption using the Brunauer-Emmett-Teller (BET) isotherm on a Micromeritics Gemini 2380.

- The crystallite structure and the quantitative composition of the phases formed during the calcination process were determined by X-ray diffraction spectroscopy (XRD, Bruker AXS D8) using the Rietveld method supported by the "Fullprof"

computer code [5, 6] under the Thompson-Cox-Hastings assumption.

- The morphology and size of particles were determined by transmission electron microscopy (TEM, JEOL JEM-1011).

- The ionic conductivities of the sintered pellets were investigated by impedance spectroscopy using a Solartron Analytical 1260 Impedance/Gain-Phase Analyzer. The data were analyzed using the "ZPlot" software (Solartron Analytical).

3 RESULTS AND DISCUSSION

3.1 Properties of the Nanopowders

TEM images of the powders up to 8YSZ are shown in Figure 1. The particles produced by the sol-gel method developed earlier by the authors are seen to be relatively well dispersed and monosized. It is possible to regulate the particle size by adjusting the calcination temperature. At the low temperature of 650°C the particles are quite small.

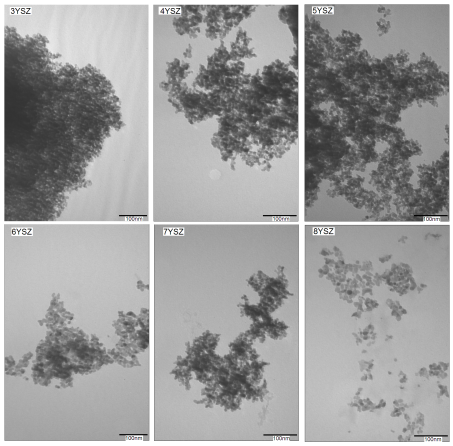

Figure 1: TEM images of the 3–8YSZ samples calcined at 650°C

The results of BET analyses of the powders are given in Figure 2, the corresponding particle sizes are calculated from the specific surface area assuming the particles to be spherical and uniformly sized. These sizes agree well with those estimated from the TEM images.

Our syntheses led to powder samples with chemical compositions in good agreement with the targeted compositions. X-ray diffraction patterns revealed a complete solid solution between ZrO_2 and Y_2O_3. The shift of the diffraction peaks as well as the powder profile refinements show that the unit-cell parameter of the cubic structure (*Fm-3m*) increases with increasing Y_2O_3 content from 5.088(8) Å in 4YSZ to 5.122(1) Å in 14YSZ.

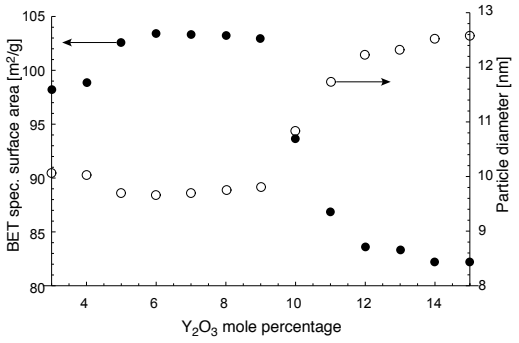

Figure 2: BET surface area and the corresponding particle size assuming the particles to be spherical and uniformly sized

Two types of structures (cubic *Fm-3m* and tetragonal *P42/nmc*) have been used for the X-ray analysis of this type of material [7]. Ghatee et al. [7] suggested that for 6.9YSZ both cubic and tetragonal phases where observed [7]. In previous studies of YSZ series only a Fm-3m cubic structure were observed for both ZrO_2 and Y_2O_3 "phases" independent of the concentration of Y_2O_3. To confirm this, a comparison between the observed and calculated 4YSZ powder patterns using both cubic and tetragonal structures was carried out. A better agreement, associated with a lower value of the Bragg Factor, was seen to result when using the cubic Fm-3m structure. A cubic structure is therefore indicated here.

The XRD analyses showed that the Zr-Zr, O-O and Zr-O distances increase monotonically with increasing Y_2O_3 content. Comparing the crystal constants with the values of Kawata et al. [8], which in this work were used to calculate the theoretical densities of the materials, there is close agreement, the crystal constant associated with the ZrO_2 "phase" being slightly lower and that associated with the Y_2O_3 "phase" slightly higher than the values of Kawata et al. The complete dataset for the crystal constant is plotted in Figure 3 together with the data of Kawata et al. It is clear from the figure that the trends in crystal constants with Y_2O_3 concentration for the present nanoparticles are very similar to the trends observed for the materials synthesized by Kawata et al. We mention that in the literature both (slight) contraction and dilation of the crystal structure of a given material when in the form of nanoparticles compared with the structure of the same material in the bulk have been reported [9, 10].

The size of the crystallites in the powder were estimated from the width of the peaks in the XRD patterns using the method of Scherrer [11]. Both ZrO_2 and Y_2O_3 peaks were used and the data agreed quite well. The results are shown in Figure 4. The crystallite size clearly decreases with increasing doping.

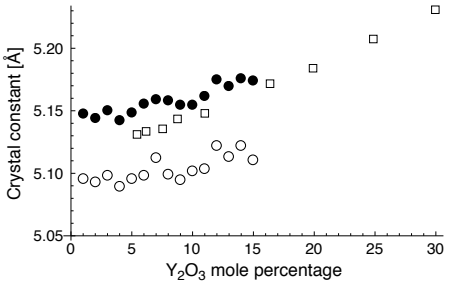

Figure 3: Data for crystal constant. The present data for the crystal constants associated with the ZrO_2 "phase" (circles) and with the Y_2O_3 "phase" (disks) compared with the data of Kawata et al. [8] (squares)

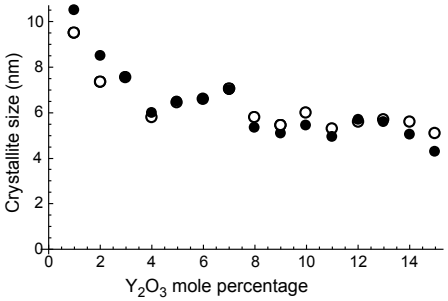

Figure 4: Data for crystallite size determined from the XRD peaks using the Scherrer formula. Results are shown for both the ZrO_2 peaks (circles) and the Y_2O_3 peaks (disks).

3.2 Properties of the Sintered Materials

After sintering the powders to pellets, the envelope density of the pellets were measured using an Archimedes principle with water as the pycnometric fluid impregnating the pellets with a hydrophobic coating to avoid the water penetrating into the pores. Using the theoretical densities calculated, as mentioned above from the crystal constants of Kawata et al. relative densities of the pellets were calculated. The results are shown in Figure. 5.

The linear shrinkage of the materials upon sintering was measured using a micrometer, this is important e.g. for the manufacture of solid oxide fuel cells. The results are shown in Figure 6. The shrinkage increases with the yttrium content.

The conductivity was characterized using EIS, electrical impedance spectroscopy, involving the application of alternating voltages with a range of frequencies over the sample and monitoring the response in terms of current obtaining both a resistivity and a time-lag between voltage and current.

Since the time-lag is very different between the grain

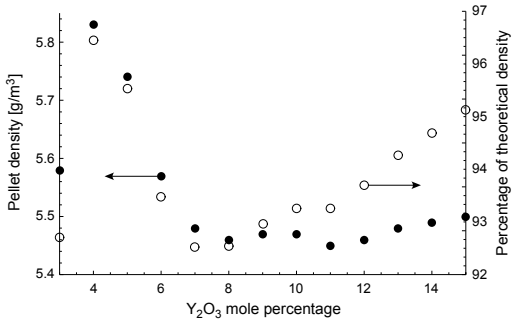

Figure 5: Densities and relative densities of YSZ pellets after sintering

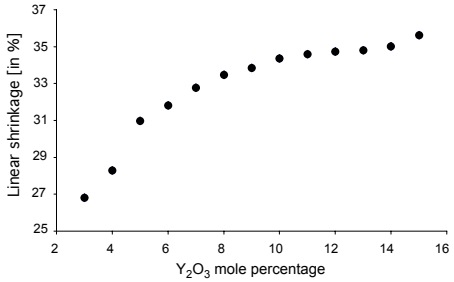

Figure 6: Linear shrinkage of the samples upon sintering

interiors and the grain boundaries of the material, it is possible to discern between the contributions of these two regions to the over-all resistivity of the material. Results for this will be presented elsewhere, here the over-all resistivity (or conductivity) will be discussed.

The results for over-all ionic conductivity are compared with literature results to obtain information as to the suitability of this material, produced by sintering from nanoparticles synthesized by a modified version of the sol-gel method, for SOFC electrolytes, which was one of the objectives of this work. To illustrate that the variation in conductivity with doping level is quite significant and at the same time to perform a stringent comparison with literature results the overall ionic conductivities are set out on a linear axis for the temperatures of 800 and 1000°C in Figure 7 together with results read off the graphically presented results of Arachi et al. [1].

The agreement is quite close. Arachi et al. do not give information about the contributions of the grain interior and grain boundaries, respectively, while the relative density of their materials is stated to be "greater than 95%". The relative densities of our materials, are given in Figure 5.

4 CONCLUSIONS

This work has elucidated the properties of xYSZ nanopowders and functional materials where x varies between 1 and 15%.

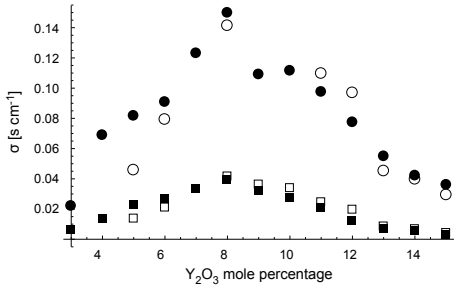

Figure 7: The overall conductivity of the present materials (filled symbols) as a function of dopant concentration at 800 and 1000°C compared with the results of Arachi et al. [1] (open symbols)

XRD data show that all the nanopowder crystal structures are cubic. The crystal constants, both associated with the Y_2O_3 phase and the ZrO_2 "phase" increase with doping level, in line with data in literature. Information about interatomic distances has been presented, all the distances, and shown to increase monotonically with doping level. Crystallite sizes are shown to decrease with increasing doping level from about 11 to about 4.5 nm. The crystallite size determined from the Y_2O_3 and the ZrO_2 XRD peaks agree well.

The relative densities of the sintered materials exhibited a minimum at around 8 mol % doping, while the linear shrinkage of the materials upon sintering increased monotonically from about 26.5% to about 36.5% with increasing doping.

Results for the over all conductivity are consistent with literature, showing that the materials produced by the new sol-gel method are suitable for use as SOFC electrolyte materials.

5 ACKNOWLEDGMENTS

The authors are grateful for funding from the NFR (Norwegian Research Council) under the NANOMAT program. The authors are also indebted to to Senioringeniør Egil Erichsen (Laboratory for Electron Microscopy, University of Bergen, Norway) for help with micrographs and to Dagfinn Mæland and Ole Thormodsæter for setting up and validating the EIS analyses.

REFERENCES

[1] Y. Arachi, H. Sakai, O. Yamamoto, Y. Takeda, and N. Imanishai. Electrical conductivity of the ZrO_2-Ln_2O_3 (Ln=lanthanides) system. Solid State Ionics, 121, 133–139, 1999.

[2] B. Butz, H. Störmer, D. Gerthsen, M. Bockmeyer, R. Krüger, E. Ivers-Tiffeé, and M. Luysberg. Microstructure of nanocrystalline yttria-doped zirconia thin films obtained by solgel processing. J. Am. Ceram. Soc., 91, 2281–2289, 2008.

[3] C. Suciu, A. C. Hoffmann, E. Dorolti, and R. Tetean. NiO/YSZ nanoparticles obtained by new sol-gel route. Chemical Engineering Journal, 140, 586–592, 2008.

[4] C. Suciu, A. C. Hoffmann, A. Vik, and F. Goga. Effect of calcination conditions and precusor proportions on the properties of YSZ nanoparticles obtained by modified sol-gel route. Chemical Engineering Journal, 138, 608–615, 2008.

[5] H. M. Rietveld. A profile refinement method for nuclear and magnetic structures. Journal of Applied Crystallography, 2, 65–71, 1969.

[6] J. Rodriguez-Carvajal, M. T. Fernandez-Diaz, and J. L. Martinez. Neutron diffraction study on structural and magnetic properties of La_2NiO_4. Journal of Physics: Condensed Matter, 33215–3234, 1991.

[7] M. Ghatee, M. M. Shariat, and J. T. S. Irvine. Investigation of electrical and mechanical properties of tetragonal/cubic composite electrolytes prepared by impregnation of 8YSZ with zirconia solution. ECS Transactions, 251541–1550, 2009.

[8] K. Kawata, H. Maekawa, T. Nemoto, and T. Yamamura. Local structure analysis of YSZ by Y-89 MAS-NMR. Solid State Ionics, 1771687–1690, 2006.

[9] W. H. Qi, P. Wang, and Y. C. Su. Size effect on the lattice parameters of nanoparticles. Journal of Materials Science Letters, 21877–878, 2002.

[10] Zhiqiang Wei, Tiandong Xia, Jun Ma, Wangjun Feng, Jianfeng Dai, Qing Wang, and Pengxun Yan. Investigation of the lattice expansion for Ni nanoparticles. Materials Characterization, 58(10)1019 – 1024, 2007.

[11] J. I. Langford and A. J. C. Wilson. Scherrer after sixty years: A survey and some new results in the determination of crystallite size. Journal of Applied Crystallography, 11102–113, 1978.